Available online at www.sciencedirect.com
SCIENCE DIRECT®
Journal of Organometallic Chemistry 690 (2005) 4939–4944
Journal of Organometallic Chemistry
www.elsevier.com/locate/jorganchem

The aromaticity of tungstenacyclobutadiene, $Cl_3W(–ButC–CMe–CMe–)$: A DFT/NICS study

Fredrick Erdman III, Daniel B. Lawson *

Department of Natural Science, University of Michigan-Dearborn, 4901 Evergreen Road, Dearborn, MI 48128-1491, United States

Received 10 May 2005; received in revised form 12 August 2005; accepted 12 August 2005
Available online 19 September 2005

Abstract

B3LYP and MP2 are used to investigate the geometry and aromaticity of tungstenacyclobutadiene, $Cl_3W(–ButC–CMe–CMe–)$. Nucleus-independent chemical shift is used as an index of aromaticity for this experimentally observed metallacyclobutadiene. Additionally, charge effects are explored by characterizing the aromaticity of the tungstenacyclobutadiene fragment ions, $WC_3H_3^{+3}$ and $WC_3H_3^{+1}$. CMO-NICS analysis provides the contribution of each B3LYP orbital to the aromaticity and allows differentiation between orbitals of σ and π symmetries.

Keywords: Metallacyclobutadiene; Transition metal heterocyclic complex; Aromaticity

1. Introduction

Metallacyclobutadienes are most noted for their role as intermediates in acetylene metathesis [1]. Additionally, these systems exhibit enough stability to have been isolated and characterized [2–4]. Metallacyclobutadienes are unsaturated planar cyclic systems analogous to cyclobutadienes and are therefore of interest due to contrasting behaviors. Cyclobutadienes are considered transiently stable at best and the lack of stability is associated with the molecule's antiaromatic nature. One of the most common considerations made to the aromaticity of planar cyclic unsaturated molecules is the number of π-electrons: the Hückel rule suggests that planar molecules with $4n + 2$ π-electrons are more stable than molecules with $4n$ π-electrons. Like cyclobutadiene, metallacyclobutadienes with 4 π-electrons could be classified as antiatromatic. Metallacyclobutadienes, however, have a high symmetry and a stability, which is atypical of antiaromatic molecules [5].

What makes the metallacyclobutadienes unique is the inclusion of d orbitals in the valance π system. There have been several theoretical studies of metallacyclobutadienes. A study by Bursten [6] exploring the relative stability and high symmetry of metallacyclobutadienes indicated that the metal's d orbitals offer greater bond formation with the p orbitals of the C atoms in the ring. Later studies by Anslyn, Brusich, and Goddard [7] and then Woo, Folga, and Ziegler [8] elaborated more on the electronic structure of metallacyclobutadiene and the energetics of the metathesis process along with conversion to metallatetrahedrane. Other than mentioning aromaticity in terms of the π electrons, neither study characterized the magnetic nature of the systems.

Recently in the work of Huang, Yang, and Li [9], a far more comprehensive study defining the aromaticity of several transition metal heterocyclic complexes was performed. They reported the aromaticity of the molecules in terms of a variety of methods including some related to magnetic character such as diamagnetic susceptibility exaltation and NMR chemical shift of out-ring protons. In this work we apply nucleus-independent chemical-shift to the four-member tungstacyclobutadiene and explore the aromatic character of the molecule in terms of orbital contributions. We wish to address the following questions: How do the σ and π electrons contribute to the aromaticity? What is the

* Corresponding author. Tel.: +1 313 593 4921.
E-mail address: dblawson@ymich.edu (D.B. Lawson).

0022-328X/$ - see front matter © 2005 Elsevier B.V. All rights reserved.
doi:10.1016/j.jorganchem.2005.08.013

effect of charge on the aromaticity of the metallacyclobutadiene core as in adding two electrons? and the related question; Does the metallacyclobutadiene ring follow the Hückel $4n + 2$ rule for aromaticity?

2. Calculation details

Energy optimized geometries and vibrational frequencies have been computed for three different tungstenacyclobutadiene systems. The first corresponds to the experimentally isolated system, Cl_3W(–ButC–CMe–CMe–), [2] and the other two systems include the metallacyclobutadiene fragments, WC_3H_3, with charges of +1 and +3. Density functional theory used in this study consisted of both the correlation functional of Lee, Yang, and Parr [10] along with Becke's three-parameter hybrid functional [11] (B3LYP). MP2 calculations were performed with four frozen core electrons. Basis sets for the W and Cl atoms included the Los Alamos effective core potential plus double zeta (LANL2DZ) [12]. For the C and H centers, either a Dunning/Huzinaga full double zeta [13] basis set (D95) was used or the standard 6-31g** basis with the polarization functions added to Cl as described in Huang, Yang, and Li [9]. We will refer to the LANL2DZ with the D95 basis on C and H as B1 and the LANL2DZ with the 6-31g** basis on Cl, C and H as B2.

NMR shielding tensors were computed with the guage-independent atomic orbital (GIAO) method [14–18] B3LYP. Nucleus-independent chemical shifts [19] (NICS) were the result of calculating the isotropic shift at the geometric center of the ring as described in the section labeled nucleus-independent chemical shift. All calculations were performed with GAUSSIAN98 [20]. The NICS of the contributions from each canonical molecular orbital (CMO-NICS) are performed using the NBO 5.0 program [21].

3. Molecular geometry

The geometry of Cl_3W(–ButC–CMe–CMe–) can be described as having a trigonal pentagonal orientation about the metal center with two of the Cl ligands occupying axial positions above and below, and the remaining Cl along with the hydrocarbon ring occupy the equatorial position. Fig. 1(a) provides the experimental bond distances along with our B3LYP/B1 and B3LYP/B2 results. Although computed gas phase bond lengths are typically longer than solid state experimental, our bond distances and angles are in good agreement those of experiment. Specifically, the experimental W–αC bond distance adjacent to the *t*-butyl group is 1.869 Å whereas the B3LYP/B1 is 1.924 Å and the B3LYP/B2 is 1.915 Å. These computed bond distances give the largest difference from experiment of 0.055 and 0.046 Å, respectively. The difference in the W–αC and αC–βC bond lengths is attributed to steric effects. For example, replacing the *t*-But with Me, for example, has little effect on the longer bond length. The B3LYP/B1 geometry optimized W–αC bond distances are 1.912 and 1.900 Å. A similar result is observed with the αC–βC as they become much closer in length, 1.467 and 1.486 Å, respective of their counter parts from Fig. 1(a). The small difference in the two pair of bonds Cl_3W(–CMe–CMe–CMe–) are attributed to the orientation of the Me attached to the βC as replacement of the Me groups with H atoms leads to system with a symmetry of C_{2v}.

The remaining computed ring bond distances of Cl_3W-(–ButC–CMe–CMe–) are no more than 0.034 Å longer than the corresponding experimental bond distances. In comparing B3LYP of the two different basis sets with experimental bond distances, the B1 basis gives slightly better C–C bond distances whereas the B2 gives better W–αC bond distances and a significantly better W–Cl bond distances. The largest B1 W–αC bond distance deviation is 0.055 Å and the largest C–C bond distance difference is 0.013 Å. The B3LYP/B1 W–equatorial Cl bond distance is 0.047 Å longer than the reported experimental value whereas the B3LYP/B2 is equivalent with experiment. The W–axial Cl bond distances are both equal and computed to be longer than the W–equatorial Cl bond distance. B3LYP/B1 and B3LYP/B2 W–equatorial Cl bond distances are 2.469 and 2.424 Å, respectively.

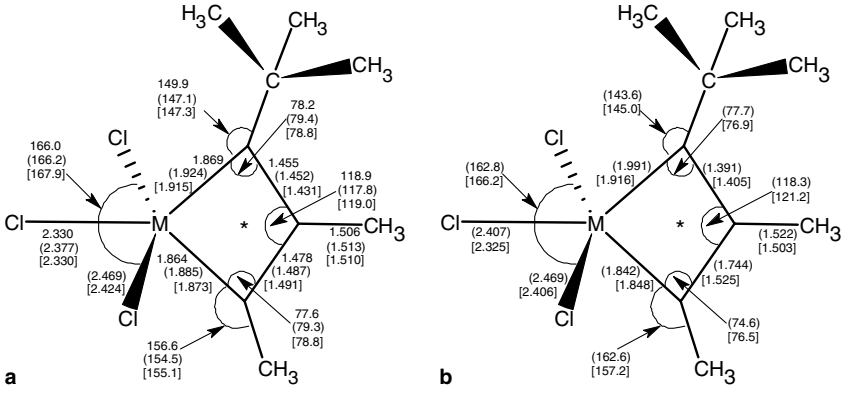

Fig. 1. (a) Experimental and calculated bond distances (Å) and angles (°) of Cl_3W(–ButC–CMe–CMe–). The top values listed are the available experimental numbers as provided in [2], B3LYP/B1 values are enclosed in parenthesis, and B3LYP/B2 values are enclosed in brackets. (b) Computed MP2 bond distances (Å) and angles (°). MP2/B1 values are enclosed in parenthesis, MP2/ B2 values are enclosed in brackets.

Fig. 1(b) gives select bond distances and angles for both basis sets at the MP2 level. Unlike the molecular geometry as reported by experiment and density functional, the resulting MP2/B1 geometry suggests localized double and single bonds between the ring atoms. The MP2/B1 W–αC bond distances are 1.991 and 1.842 Å and the αC–βC bond distances are 1.391 and 1.744 Å. The MP2/B2 is closer to those of B3LYP and experiment as the W–αC bond distances are 1.916 and 1.848 Å, and both αC–βC bond distances are 1.405 and 1.525 Å. By comparison with the B1 basis set, B2 significantly improves the bond distances at the MP2 level. However, relative to the DFT used in this study, MP2 under-emphasizes the delocalization. The MP2/B2 difference between the 2 αC–βC bonds in the ring is 0.120 Å whereas the difference in the B3LYP/B2 ring αC–βC bond distances is 0.060 Å. The αC–βC bond distance distortion in the MP2/B1 is even more pronounced where the difference is 0.353 Å. The MP2/B1 W-equatorial Cl bond distance is 2.407 Å or 0.077 Å longer than the reported experimental value, whereas, the MP2/B2 is W-equatorial Cl bond distance is 0.005 A shorter than the reported experimental value. As with B3LYP, the MP2 W-axial Cl bond distances are both longer than the W–equatorial Cl bond distance. MP2/B1 and MP2/B2 W–equatorial Cl bond distances are 2.488 and 2.406 Å, respectively. Although not reported here, the computed vibrational frequencies with this MP2 geometry are all non-imaginary.

The aromaticity of the tungstenacyclobutadiene depends on the nature of the electronic structure of the WC_3H_3 ring. In this work, we explore the singlet states of both the $WC_3H_3^{+3}$ and the $WC_3H_3^{+1}$ fragment ions. The computed geometries, total energies, zero point vibrational energies, and NICS values for the +1 and +3 fragment ions are presented in Fig. 2. Geometry optimizations with both B3LYP/B1 and B3LYP/B2 for $WC_3H_3^{+3}$ were initially performed without symmetry and converged to a structure indicating C_{2v} where bond distances were within 0.001 Å and bond angles where within 0.001° of C_{2V} symmetry. W–αC bond distances of 1.881 and 1.860 Å and αC–βC bond distances of 1.524 and 1.490 Å, respective of the method and basis sets. Geometry optimizations with B3LYP/B1 and the B3LYP/B2 $WC_3H_3^{+1}$ also converged to a symmetry of C_{2V},with similar tolerances listed above, with W–αC bond distances of 1.895 and 1.867 Å and αC–βC bond distances of 1.455 and 1.437 Å, respectively. The αC–βC bond distances suggest that the $WC_3H_3^{+1}$ also better represents the electronic structure of the ring in Cl_3W(–ButC–CMe–CMe–). The W–αC bond distance changes little from the +1 ion to the +3 and we address this below.

4. Nucleus-independent chemical-shift

The aromaticity of the organometallic rings of this study are characterized in terms of NICS. NICS is a simple probe of aromaticity determined by calculating the absolute magnetic shielding at a location within the aromatic part of the molecule, typically the center of the ring [19]. Negative values of NICS indicate a diatropic ring current in the presence of an applied magnetic field whereas a positive NICS value indicates a paratropic ring current. A diatropic ring current manifests itself experimentally as a low-field shift in the NMR of the exocyclic protons, consistent with aromatic molecules. By contrast, a paratropic ring current corresponds to a high-field shift in the NMR consistent with antiaromatic molecules. In summary, a negative NICS indicates an aromatic molecule whereas a positive NICS indicates an antiaromatic molecule.

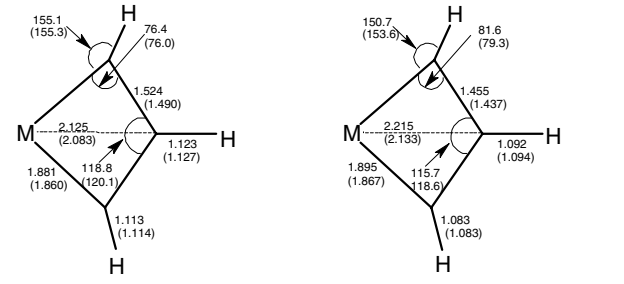

Singlet, +3, C_{2v}

Energy	ZPE	NICS(0)
-182.2070	0.0419	+23.8
(-182.2451)	(0.0452)	(+14.9)

Singlet, +1, C_{2v}

Energy	ZPE	NICS
-183.4705	0.0453	-135.4
(-183.4987)	(0.0451)	(-138.7)

Fig. 2. Geometries, energies, zero point energies and NICS of the tungstenacyclobutadiene ions. B3LYP/B1 bond distances and angles are the top values, whereas, the B3LYP/B2 numbers are enclosed in parenthesis.

NICS values were taken at a location near the geometrical center of the ring. Typically, NICS is taken at the mass weighted center of the molecule [19], however, due to both the large mass and electronic extent of the WCl_3 fragment relative to the C_3H_3 fragment, NICS was taken at the geometric center of the ring. The geometric center of the ring was chosen as the intersection of the line between the two αC and the line connecting the metal with the βC indicated by the asterisk in Fig. 1. We chose the geometric center of the ring as the location of NICS as it is closer to the center of the aromaticity of the ring. Furthermore, the electronic extent of the metal's electrons cause NICS fluctuate significantly near the nuclear centers. A more thorough justification for this choice of center can be found in Appendix A.

The B3LYP/B1 NICS value of Cl_3W(–ButC–CMe–CMe–) was calculated to be −28.0 ppm whereas B3LYP with the B2 basis gives a slightly larger NICS value of −31.6 ppm. Even though the geometry is significantly distorted suggesting localized bonding in the ring, MP2/B1 NICS is −24.9 and the MP2/B2 NICS is slightly more diatropic with a value of −29.1 ppm. NICS confirms the aromaticity of tungstenacyclobutadiene.

5. Charge and aromaticity

The aromaticity of molecules such as cyclobutadiene, benzene, and their ions follow the Hückel $4n + 2$ rule, in that, addition or removal of pairs of electrons toggles

a system between aromatic and antiaromatic. As such, all properties associated with aromaticity should toggle along with the number of π electrons. The valence electrons of these planar unsaturated hydrocarbons are dominated by π orbitals from which the Hückel $4n + 2$ rule is derived. Adding or removing pairs of electrons from transition-metal metallacycloalkenes, however, would suggest a more sophisticated treatment for the determination of aromaticity as the d orbitals from the metal center interact differently then do s and p orbitals.

Initially, it might seem sensible to model Cl_3W(–ButC–CMe–CMe–) with a +2 charge when considering the Hückel $4n + 2$ rule. The dilemma, however, is that the positive 2 charge is distributed throughout the molecule. In a B3LYP/B1 calculation, the charge on the metal center of Cl_3W(–ButC–CMe–CMe–)$^{+2}$ is +1.14 whereas the charge on the metal in the neutral species is +0.80. The sum of the charges on the three Cl ligands goes from −0.04 in the positive two species to −0.81 in the neutral. These calculations indicate that the overall charge on the ring in the neutral Cl_3W(–ButC–CMe–CMe–) is closer to +1 rather than the +3 as would be predicted by formally counting electrons. Therefore, the $[W(C_3H_3)]^{+1}$ is a better model of the electronic structure of the title system then is $[W(C_3H_3)]^{+3}$. However, to help understand the orbital and charge effects on the aromaticity of the metallacyclobutadiene ring, we look to both WC_3H_3 fragment ions.

NICS calculations for the $WC_3H_3^{+1}$ fragment ion indicate the system to be aromatic as the B3LYP/B1 and the B3LYP/B2 NICS are both diatropic, −135.4 and −138.7, respectively. The B3LYP/B1 and the B3LYP/B2 NICS, however, indicate $WC_3H_3^{+3}$ to be paratropic overall with values of +23.8 and +14.9, respectively. The $WC_3H_3^{+1}$ fragment ion is aromatic whereas the $WC_3H_3^{+3}$ fragment ion is antiaromatic, yet the geometries of these fragment ions are very similar. Antiaromatic molecules are thought to have adjacent bond distances that alternate between single and double [22], however, this is not the case in the $WC_3H_3^{+3}$ fragment ion. In comparing the bond distances of $WC_3H_3^{+1}$ and $WC_3H_3^{+3}$ there is only a relatively small differences in the structure of the ions. The B3LYP/B1 W–αC bond is 0.014 Å longer in $WC_3H_3^{+1}$ than the corresponding bond distance of $WC_3H_3^{+3}$ whereas the αC–βC bond distance is 0.069 Å shorter between the respective fragment ions.

To understand these results Figs. 3 and 4 contain the B3LYP/B1 CMO-NICS analysis of both $WC_3H_3^{+3}$ and $WC_3H_3^{+1}$, respectively. From Fig. 3, both the σ and π electrons of $WC_3H_3^{+3}$ are paratropic overall. The highest three σ molecular orbitals are diatropic, whereas the lower σ orbitals shown are diatropic. The core orbitals contribute little. It is the HOMO-2(σ) orbital making the largest paratropic contribution of +30.6. The HOMO of the system is a π orbital and is paratropic, +49.1 ppm. The HOMO-3π is the second highest π orbital, and this delocalized orbital is diatropic in nature, −30.4 ppm.

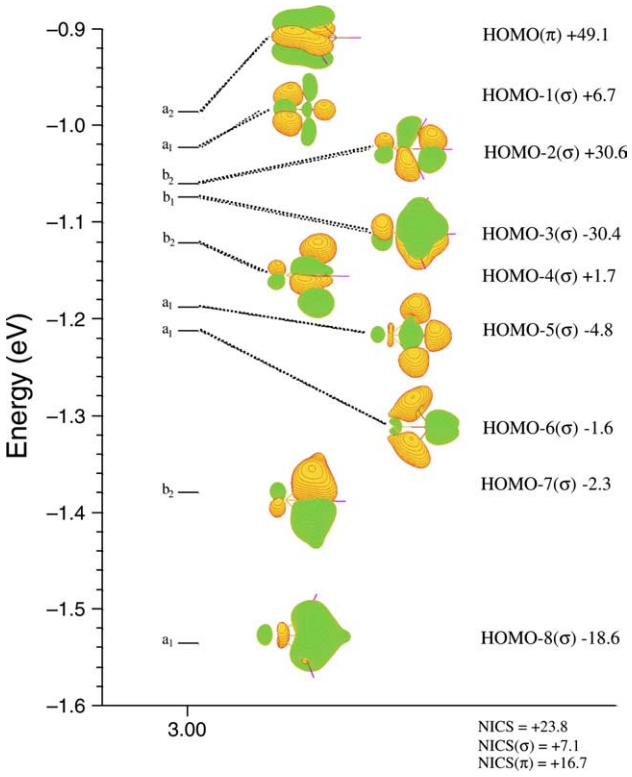

Fig. 3. NBO CMO-NICS analysis at the $WC_3H_3^{+3}$ center.

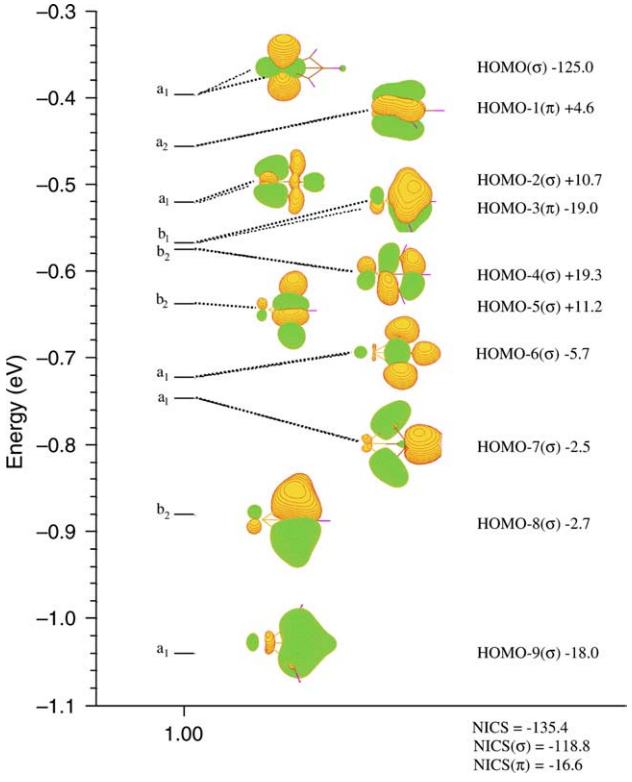

Fig. 4. NBO CMO-NICS analysis at the $WC_3H_3^{+1}$ center.

Fig. 4 indicates the $WC_3H_3^{+1}$ ring to be both σ and π diatropic, −118.0 and −16.6 ppm, respectively. The relative ordering of the orbitals in $WC_3H_3^{+1}$ is the same as in

$WC_3H_3^{+3}$ with the exceptions of the HOMO-2 and HOMO-3 and, of course, an additional pair of electrons. The HOMO is a lone pair of electrons localized almost completely on the W metal center. From the CMO-NICS analysis, this lone pair orbital makes the largest single diatropic contribution of −125.0 ppm. Elimination of the contribution of this orbital leaves the σ space paratropic, however, the ion is still diatropic overall. As for the π aromaticity of the fragment ions, the primary difference according to NICS is in the contribution of the π-HOMO. The a_2 orbital of both ions is paratropic, however, the magnitude of the orbital in $WC_3H_3^{+1}$ is substantially reduced relative to the same orbital in $WC_3H_3^{+3}$. This a_2 orbital is a localized orbital between the metal and the two αC atoms. The π bonding is equivalent along both W–αC bonds and does not cause alternation between adjacent bonds as in typical antiaromatic hydrocarbon rings.

One interpretation of the alternation between single and double bonds, as in antiaromatic hydrocarbon molecules, has been attributed to the π electron distortion of an otherwise symmetric σ electron backbone [23]. The π space of the either WC_3H_3 fragment ions is surprisingly analogous to cyclobutadiene. Fig. 5 provides a schematic of the π orbitals of both tungstenacyclobutadiene and cyclobutadiene. In both systems there are two π orbitals in the valence space. The lower energy π orbital is completely delocalized around the ring whereas the higher energy π orbital is localized on two non-adjacent bonds. Unlike cyclobutadiene, however, both phases of the π-HOMO in either of the WC_3H_3 fragment ions are centered on the W. Therefore, in comparing the $WC_3H_3^{+3}$ with the $WC_3H_3^{+1}$ ion, adding two electrons shifts the system from antiaromatic to aromatic, however, the bond distances do not necessarily follow in a manner consistent, for example, with C_4H_4 and $C_4H_4^{+2}$. Our description of the a_2 is not unlike those given by Bursten [6] or Bleeke [24], however, here the a_2 orbital is deemed antiaromatic and localized.

6. Conclusions

B3LYP calculated bond distances of Cl_3W(–ButC–CMe–CMe–) are in good agreement with those of experiment, however, the computed bond distances between the ring atoms are distorted by comparison with the equivalent observed bond distances. Since NICS indicates Cl_3W(–ButC–CMe–CMe–) to be aromatic regardless of method or basis used in this study, the small bond distance alternation in Cl_3W(–ButC–CMe–CMe–) is due to steric effects of the functional groups attached to the ring C atoms. MP 2 bond distances appear to suffer from bond distance alternation more than B3LYP.

NICS of the fragment ions indicates $WC_3H_3^{+3}$ to be antiaromatic whereas $WC_3H_3^{+1}$ is aromatic. Although the $WC_3H_3^{+3}$ fragment ion is antiaromatic, the bonding is equivalent between the two W–αC bonds resulting in a symmetric ring. The HOMO of $WC_3H_3^{+1}$ is a non-bonding orbital localized on the W center, whereas the HOMO of the $WC_3H_3^{+3}$ is a bonding orbital localized between the W center and the two αC atoms. Considering the difference in charge, the resulting deviation in bond distances between the +1 and the +3 is surprisingly small. Finally, since both $WC_3H_3^{+1}$ and $WC_3H_3^{+3}$ have 4π electrons, the Hückel $4n + 2$ rule is not a simple function of charge. To evaluate the aromaticity of systems involving d electrons, contributions of both the σ and π electrons must be explicitly considered.

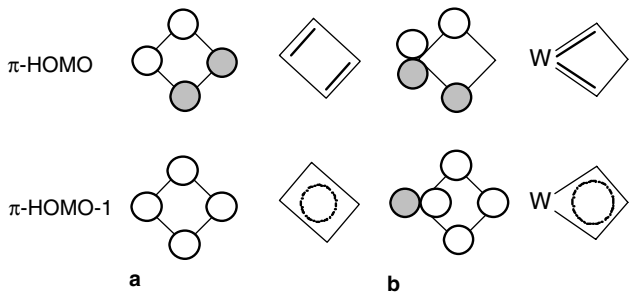

Fig. 5. Schematics of the π-HOMO and π-HOMO-1 of (a) cyclobutadiene and (b) tungstenacyclobutadiene.

Acknowledgment

This work was supported by a University of Michigan Rackham Faculty Grant.

Appendix A

Typical NICS values are taken at the mass weighted center of the molecule [19] or sometimes taken at a distance of 2 Å above mass weighted center [25]. In the case of metallocycles, however, the large mass of the metal relative to the C atoms of the ring places the mass weighted center close to metal atom. And of particular interest with Cl_3W(–ButC–CMe–CMe–) the mass of the Cl atoms put the mass weighted center very close to W. Although the sensitivity of NICS drops off dramatically with distance [26], the effects of the nuclear environment on NICS overwhelms any contributions associated with ring currents. We illustrate these effects in Figs. 6 and 7. Fig. 6 includes plots of NICS taken on a line along the C_2 axis of the molecules pyrrole and borol. Systems considered aromatic and antiaromatic, respectively. Our NICS values taken at the mass weighted center for both pyrrole (−15.7) and borol (+20.2) are consistent with those reported in [19]. Note, near either the B or C center, NICS is significantly negative. The value of NICS is primarily a function of the B and N nuclear environments up to and over 0.5 Å away. Similar plots are provided in Fig. 7 for our model systems $[W(C_3H_3)]^{+1}$ and $[W(C_3H_3)]^{+3}$. In both figures, NICS is large and positive near the W nucleus. The effects of the W electrons do not diminish until 0.5 Å beyond the ions mass weighted center. Both Figs. 6 and 7 indicate NICS taken near the geometric center of the ring as an appropriate location for evaluation of aromaticity.

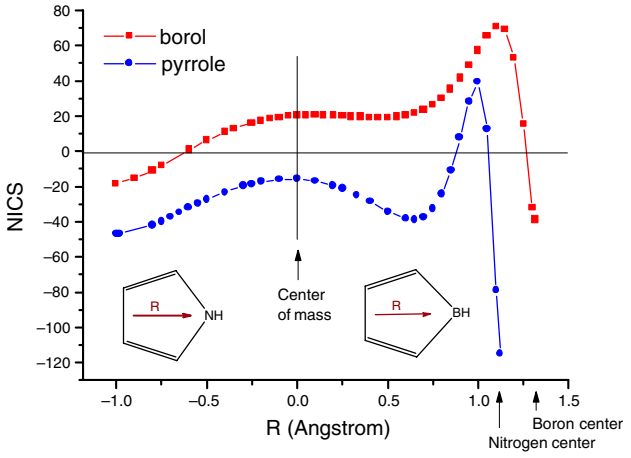

Fig. 6. A plot of B3LYP/6-31g* NICS calculated along the C_2 axis of boral and pyrrole.

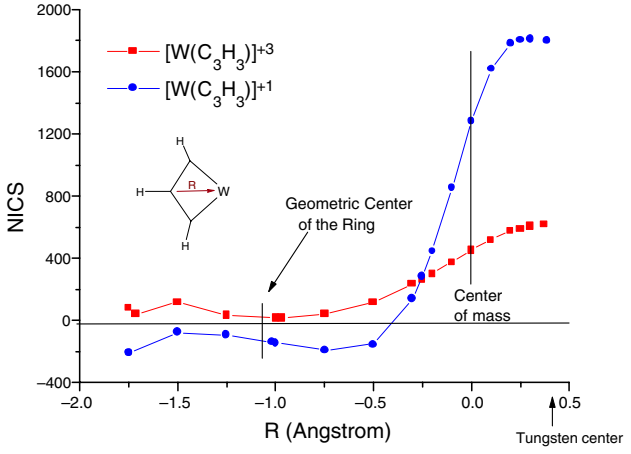

Fig. 7. A plot of B3LYP/B1 NICS calculated along the C_2 axis of $[W(C_3H_3)]^{+3}$ and $[W(C_3H_3)]^{+1}$.

References

[1] T.J. Katz, J. McGinnis, J. Am. Chem. Soc. 97 (1997) 1592.

[2] S.F. Pedersen, R.R. Schrock, M.R. Churchill, H.J. Wasserman, J. Am. Chem. Soc. 104 (1982) 6808.

[3] M.R. Churchill, J.W. Ziller, J.H. Freudenberger, R.R. Schrock, Organometallics 3 (1984) 1554.

[4] J.H. Freudenberger, R.R. Schrock, R.M. Churchill, A.L. Reingold, J.W. Ziller, Organometallics 3 (1984) 1563.

[5] A.L. Lugo, J. Fischer, D.B. Lawson, J. Mol. Struct. (Theochem) 674 (2004) 139.

[6] B.E. Bursten, J. Am. Chem. Soc. 105 (1983) 121.

[7] E.V. Anslyn, M.J. Brusich, W.A. Goddard, Organometallics 7 (1988) 98.

[8] T. Woo, E. Folga, T. Ziegler, Organometallics 12 (1993) 1289.

[9] Y.Z. Huang, S.Y. Yang, X.Y. Li, J. Org. Metal. Chem. 689 (2004) 1050.

[10] C. Lee, W. Yang, R.G. Parr, Phys. Rev. B 37 (1988) 785;
B. Miehlich, A. Savin, H. Stoll, H. Pruess, Chem. Phys. Lett. 157 (1989) 200.

[11] A.D. Becke, J. Chem. Phys. A 98 (1993) 5648.

[12] P.J. Hay, W.R. Wadt, J. Chem. Phys. 82 (1985) 299.

[13] T.H. Dunning Jr., P.J. Hay, in: H.F. SchaeferIII (Ed.), Modern Theoretical Chemistry, vol. 3, Plenum, New York, 1976, p. 1.

[14] K. Wolinski, J.F. Hilton, P. Pulay, J. Am. Chem. Soc. 112 (1990) 8251.

[15] J.L. Dodds, R. McWeeny, A. Sadlej, J. Mol. Phys. 41 (1980) 1419.

[16] R. Ditchfield, Mol. Phys. 27 (1974) 789.

[17] R. McWeeny, Phys. Rev. 126 (1962) 1028.

[18] F. London, J. Phys. Radium Paris 8 (1937) 397.

[19] P.v.R. Schleyer, C. Maerker, A. Dransfeld, H. Jiao, N.J.R.v.E. Hommes, J. Am. Chem. Soc. 118 (1996) 6317.

[20] M.J. Frisch, G.W. Trucks, H.B. Schlegel, P.M.W. Gill, B.G. Johnson, M.A. Robb, J.R. Cheeseman, T. Keith, G.A. Petersson, J.A. Montgomery, K. Raghavachari, M.A. Al-Laham, V.G. Zakrzewski, J.V. Ortiz, J.B. Foresman, J. Cioslowski, B.B. Stefanov, A. Nanayakkara, M. Challacombe, C.Y. Peng, P.Y. Ayala, W. Chen, M.W. Wong, J.L. Andres, E.S. Replogle, R. Gomperts, R.L. Martin, D.J. Fox, J.S. Binkley, D.J. Defrees, J. Baker, J.P. Stewart, M. Head-Gordon, C. Gonzalez, J.A. Pople, Gaussian 98, Gaussian, Inc., Pittsburgh, PA, 1997.

[21] NBO 5.0. E.D. Glendening, J.K. Badenhoop, A.E. Reed J.E. Carpenter, J.A. Bohmann, C.M. Morales, F. Weinhold, Theoretical Chemistry Institute, University of Wisconsin, Madison, WI, 2001. Available from: <http://www.chem.wisc.edu/~nbo5>.

[22] T.M. Krygowski, M.K. Cyrañski, Z. Czarnocki, G. Häfelinger, A.R. Katritzky, Tetrahedron 56 (2000) 1783.

[23] K. Jug, A.M. Köster, J. Am. Chem. Soc. 112 (1990) 6772.

[24] J.R. Bleeke, Chem. Rev. 101 (2001) 1205.

[25] Y. Xie, P.R. Schreiner, H.F. Schaefer III, X-W. Li, G.H. Robinson, J. Am. Chem. Soc. 118 (1996) 10635.

[26] P.v.R. Schleyer, M. Manoharan, Z. Wang, B. Kiran, H. Jiao, R. Puchta, N.J.R.v.E. Hommes, Org. Lett. 3 (2001) 2465.